ADVANCED HEALTHCARE MATERIALS
www.advhealthmat.de

Wireless and Flexible Skin Moisture and Temperature Sensor Sheets toward the Study of Thermoregulator Center

*Yuyao Lu, Yusuke Fujita, Satoko Honda, Shin-Hsin Yang, Yan Xuan, Kaichen Xu, Takayuki Arie, Seiji Akita, and Kuniharu Takei**

A disorder in the thermoregulator center in a human body leads to some potential diseases such as fever and hyperthyroidism. To predict these diseases early, monitoring the health condition of the human body due to the influence of thermoregulation disorders is important. Although extensive works are performed on sweat-rate detection by constructing microfluidic channels, skin-moisture evaporation before sweating remains unknown. This work proposes a wireless and flexible sensor sheet to investigate the thermoregulatory responses of different people under cold stimulation and exercise by measuring the temperature and moisture variations on the finger skin. An integrated flexible sensor system consists of a $ZnIn_2S_4$ nanosheet-based humidity sensor and carbon nanotube/SnO_2 temperature sensor. The results exhibit distinct thermoregulation abilities of five volunteers. Interestingly, the sudden increase in finger moisture that results from the excitation by the sympathetic nerve is observed during the cold-stimulus test. Although further studies are required to predict the potential diseases resulted from thermoregulation disorders in human body, this study provides a possibility of continuous and real-time monitoring of thermoregulatory activities via skin moisture and temperature detection using a flexible sensor sheet.

1. Introduction

Skin not only plays a significant role in protecting internal organs but also endows our body with strong thermoregulation ability and various sensory features that allow humans to quickly respond to changes in the external environment.[1–4] An autonomic thermoregulatory response of our body is necessary to maintain a stable body temperature to survive.[5,6] Usually, our body temperature is regulated in two ways: one is heat production by muscle contraction and the other is heat dissipation through the sweat glands.[7] Whether in cold environments or during exercises, the muscles involuntarily work to generate heat by thermogenesis.[8] In contrast, to balance the core temperature of our body, excess heat is gradually dissipated outside the body via sweating. Once the heat-dissipation process is upset, the body cannot normally function because of the high heat loads, which are often observed in diseases such as fever and hyperthyroidism. However, heat loss from the skin not only occurs during the thermoregulation process but is also affected by the activities of the nerve systems.[9] When human being experience high mood swings or cold stimuli, the skin also shows high moisture evaporation as a form of heat loss due to the excitation of the sympathetic nerves. During the thermoregulation process, skin temperature also plays a key role in reflecting the trends of heat production due to heat transfer from the body core to the skin via blood flow. Thus, studying the thermoregulation process of a human body is important by continuously and simultaneously monitoring the humidity and temperature on the skin surface. For this measurement, finger skin, which is endowed with a unique fingerprint structure and high sensitivity to environmental changes, is considered as one of the most suitable places for monitoring body reaction to external and internal stimuli.[10] Furthermore, the highly dense nerve distribution on the finger skin allows it to quickly recognize the size and textures of the touched object.

Many recent works have succeeded in studying the sweat rate of human beings under different physical activities by constructing microfluidic channels.[11,12] However, determining the start of heat dissipation using this type of system remains difficult because sweat formation requires a long time. In fact, an increase in heat loss occurs at the beginning of running, whereas sweat takes time to produce. In addition, when people feel nervous or wakeful owing to some stimuli, no evident sweat is produced, but the moisture evaporation from skin invisibly increases because of the secretion by sweat glands resulting from sympathetic excitation.[13] Electrodermal tests have been

Y. Lu[+], Y. Fujita, S. Honda, S.-H. Yang, Y. Xuan, Prof. K. Xu[+], Prof. T. Arie, Prof. S. Akita, Prof. K. Takei
Department of Physics and Electronics
Osaka Prefecture University Sakai
Osaka 599-8531 Japan
E-mail: takei@pe.osakafu-u.ac.jp
Prof. K. Takei
JST PRESTO
Kawaguchi Saitama 332-0012, Japan

The ORCID identification number(s) for the author(s) of this article can be found under https://doi.org/10.1002/adhm.202100103

[+]Present address: State Key Laboratory of Fluid Power and Mechatronic Systems, School of Mechanical Engineering, Zhejiang University, Hangzhou 310027, China

DOI: 10.1002/adhm.202100103

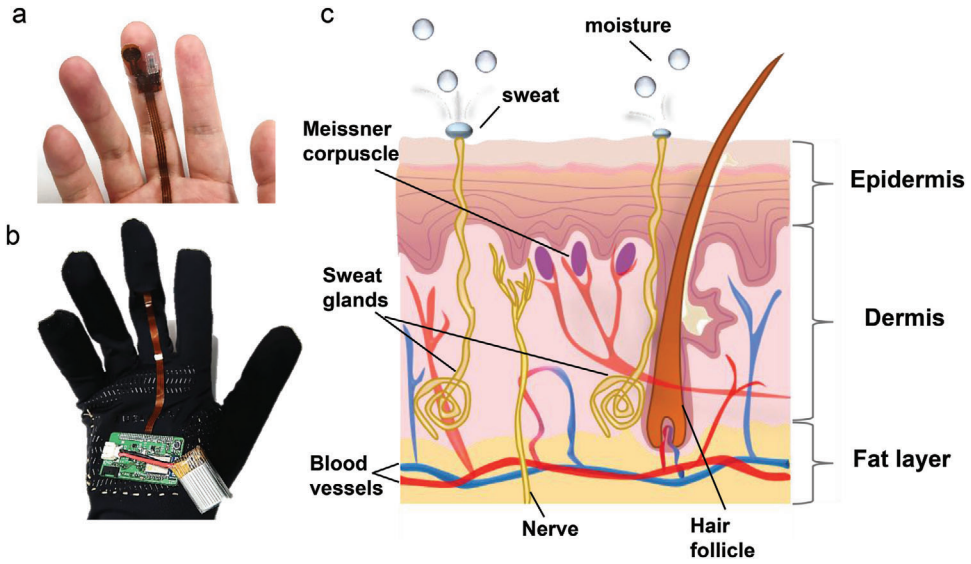

Figure 1. a) Photograph of the integrated device on a bare finger. b) Photograph of the glove-based device with wireless connection. c) Schematic picture of a finger-skin structure.

widely performed to investigate human-emotion changes by measuring the skin-resistance change caused by vasodilation and contraction of blood vessels in the skin as well as by sweat secretion. However, this method uses relatively large equipment, which is not applicable for wearable applications in human activities such as working and exercising.[9,14]

To overcome this drawback, this study proposes a flexible integrated humidity and temperature sensor, which is fabricated using stacked $ZnIn_2S_4$ nanosheets and a mixture of carbon nanotube (CNT) and SnO_2, respectively, to realize both thermal and moisture detections. In particular, this study aims to continuously monitor the finger-skin temperature and moisture variation under a cold stimulus and during running using the proposed integrated wireless flexible sensor system. Both the $ZnIn_2S_4$ humidity sensor[15,16] and CNT/SnO_2 temperature sensor[17] feature commendable stability, which guarantee good performance for long-time monitoring. The ZIS humidity sensor is fabricated with porous graphene electrodes, which are produced by laser scanning process. Compared to other convenient fabrication methods, such as inkjet-printing and screen-printing, laser direct writing is the only way to create porous graphene electrodes directly.[18,19] Interestingly, this sensor system has successfully captured the reduction process in finger-skin temperature as well as the sudden increase in finger moisture under a cold stimulus when a volunteer moved from a warm to a cold room, whereas no evident moisture change was observed in the opposite process.[20–22] To confirm this result, five volunteers were invited to repeatedly perform the same experiment at a temperature difference of 8 °C. Similar responses from the five volunteers proved that a higher density of cold receptors than thermal receptors is distributed in the human body.[23–26] Furthermore, dynamic finger temperature and moisture variations were recorded during the running experiment of the five volunteers.

2. Results and Discussion

The real-time study on finger-skin moisture at different physical states was conducted by attaching the proposed integrated flexible sensor system, which included temperature and humidity sensors, on the fingers or in wearable gloves (**Figure 1**a,b).[27,28] Skin, which is endowed with complex sensory systems, not only acts as the first line of defense from external factors but also plays a major role in mechanical contact, somatic perception, and nutrient exchange with the external environment (Figure 1c).[2]

Among these features, skin wetness is an important signal that reflects the physiological and neurological activities of a human body. Normally, much skin moisture is produced to balance the body temperature when people continuously stay in a hot environment or perform physical activities, which can also be considered a heat-dissipation process for self-protection. In addition, when a person is physically stimulated or in high mood swings, such as nervousness, skin moisture exhibits upward changes owing to the hyperactivity of the sympathetic nerves. To study the finger-moisture variations, a resistive nanosheet-based humidity sensor was fabricated via depositing $ZnIn_2S_4$ nanosheets on laser-induced porous graphene (LIG) electrodes (**Figure 2**a).

As explained for most humidity sensors, the sensing mechanism of the ZIS humidity sensor is also based on a proton-hopping process between H_3O^+ ions and water molecules, in which the highest energy occupied molecular orbital–lowest energy unoccupied molecular orbital (HOMO–LUMO) gap of this semiconductor material is reduced, leading to an enhanced current level (Figure 2b).[15] The surface morphology of the ZIS nanosheets and LIG electrodes are shown in Figure 2c,d and Figure S1 in the Supporting Information, respectively. The high porosity of the graphene electrodes provides sufficient interspace for water adsorption and desorption through the ZIS nanosheet surface, resulting in better and stable humidity response, as we

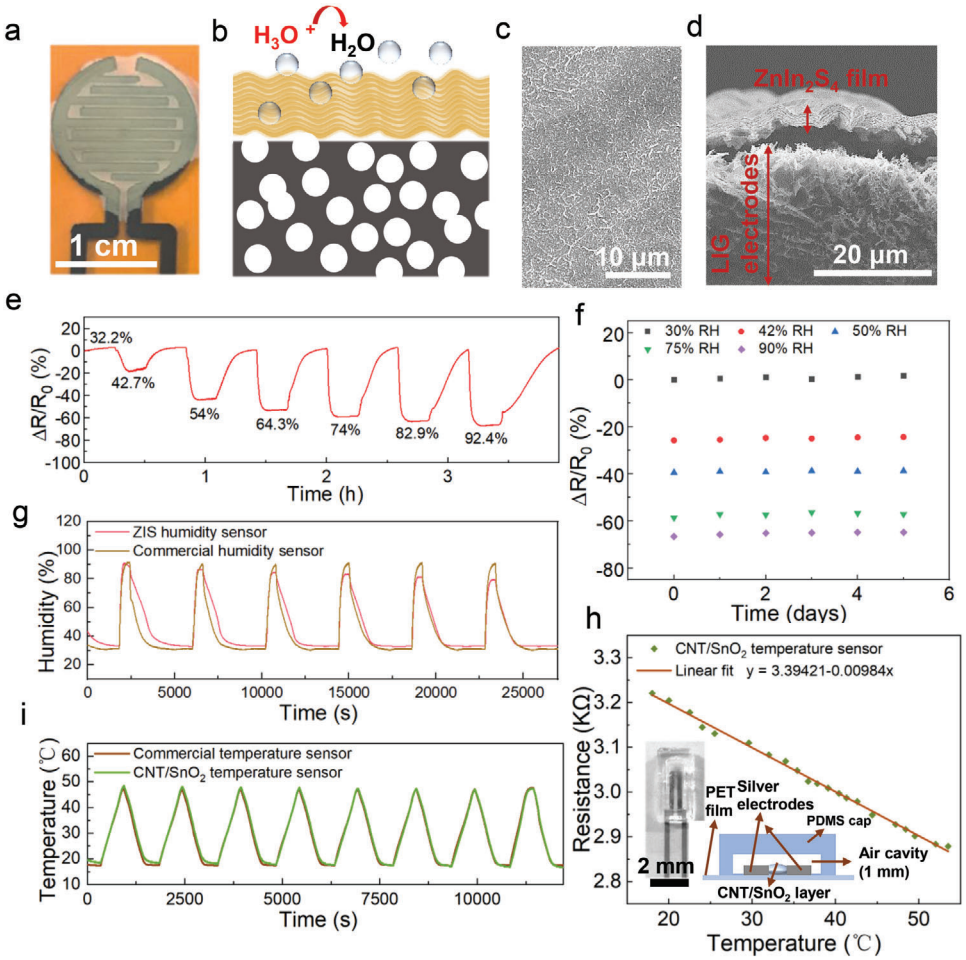

Figure 2. a) Device photograph and b) schematic of the ZIS humidity sensor. SEM images of c) surface morphology of the ZIS nanosheets and d) cross-sectional view of the ZIS nanosheets on porous graphene electrodes. e) Resistance-change ratio in the ZIS humidity sensor at different RH levels. f) Storage stability of the ZIS humidity sensor in 5 days. g) Long-time cyclic measurement of the ZIS and commercial humidity sensors. h) Device photographs and sensitivity test of the CNT/SnO_2 temperature sensor for a temperature variation from 18 to 53.5 °C. i) Long-time cyclic measurement of the CNT/SnO_2 temperature sensor calibrated using a commercial temperature sensor.

have previously reported.[15] To confirm the crystal structure of the ZIS nanosheets, Raman characterization was conducted. Raman peaks were appeared at 247, 298, 341, and 367 cm^{-1}, which belong to the longitudinal mode (LO_1), transverse optical mode (TO_2), longitudinal mode (LO_2), and A_{1g} mode, respectively (Figure S2, Supporting Information).[29]

Next, the humidity-sensing property of the ZIS sensor was characterized by measuring the resistance change at different relative humidity (RH) levels in a humidity- and temperature-controllable oven. Figure 2e shows that the humidity sensor displayed a resistance change of ≈20% when the RH varied from 32.2% to 42.7%. Subsequently, the resistance-change value kept increasing at higher humidity levels (42.7–92.4%), which verified the wide detection range of the ZIS humidity sensor. To precisely evaluate the performance of the humidity sensor, other interference factors such as temperature and device deformation were also studied. The result of the ZIS humidity sensor demonstrated a negligible effect of the temperature, although a minute resistance change (≈2%) was observed as the temperature increased from 40 to 50 °C (Figure S3a, Supporting Information). In addition, this device also exhibited good mechanical stability at different bending radii because of the wrinkled surface structure and good connection of the stacked nanosheets (Figure S3b, Supporting Information). Figure 2f shows the storage stability of the ZIS humidity sensor under different RH levels in 5 days during which the resistance change only exhibited slight fluctuations at high humidity levels (>75% RH). Furthermore, to ensure repeatability of the humidity-sensor performance in real-time monitoring applications, a cycle test was conducted. Figure 2g shows that a comparison with the cyclic behavior of a commercial humidity sensor revealed that the ZIS humidity sensor exhibited a relatively good stability at 90% RH for a long-time continuous measurement. To further confirm the stability of ZIS humidity sensor with a waterproof and breathable membrane filter, another cycle test at a humidity range of 35–58% was also successfully investigated (Figure S4, Supporting Information). In our previous work, the response time and recovery time of ZIS humidity sensor were characterized (response time: 1 s; recovery time: 22 s).[15] It should be noted that the output behavior gradually degraded because of the high humidity-level

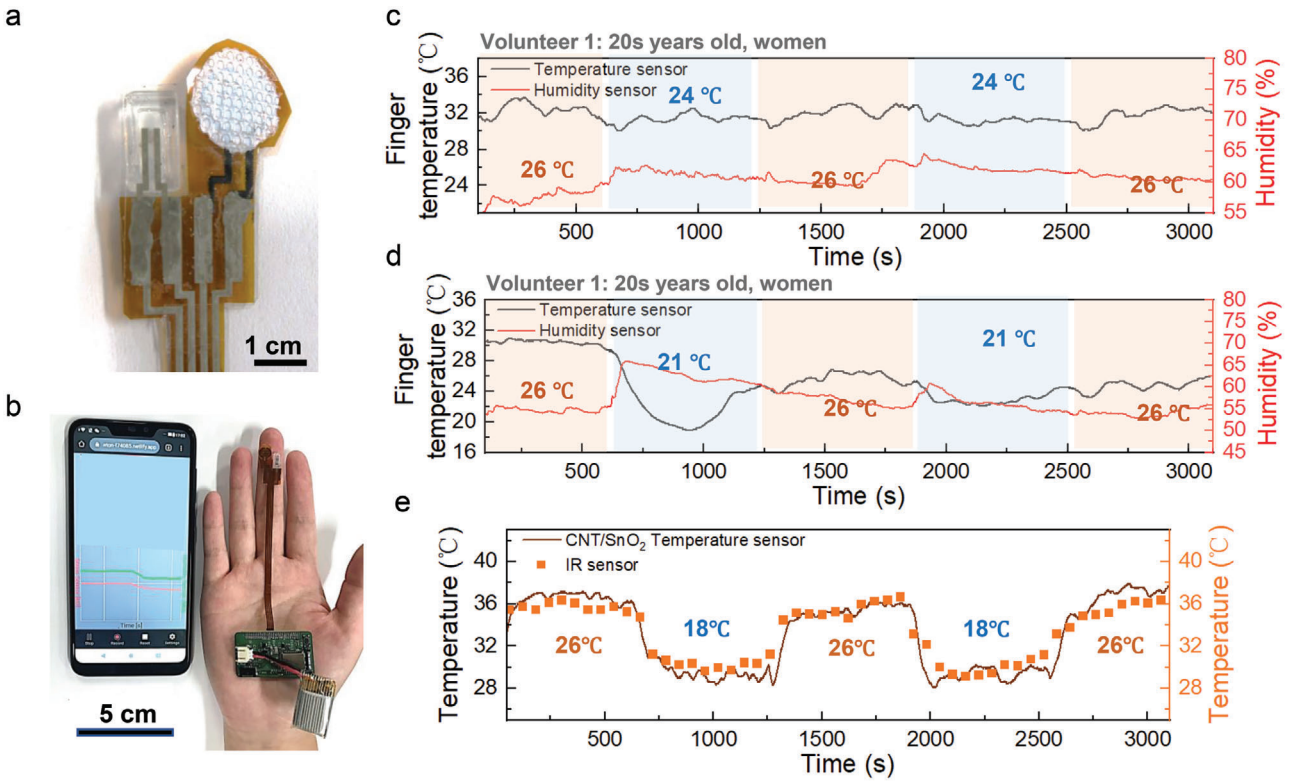

Figure 3. a) Photograph of the integrated device with a ZIS humidity sensor and a CNT/SnO_2 temperature sensor. b) Image of the wireless sensor system for finger temperature and moisture detection. Real-time monitoring results of the finger temperature and moisture variations of a volunteer who moved between a warm and a cold room with a temperature difference of c) 2 and d) 5 °C. e) Calibration result of the CNT/SnO_2 temperature sensor utilizing a thermal IR imager when the volunteer was subjected to a temperature difference of 8 °C.

measurement, this trend agreed well with the results shown in Figure 2f.

Flexible temperature sensor is also an essential part of a wearable device that can conveniently and continuously detect skin temperature. To determine the relationship between the finger-moisture level and skin temperature during human activities, a flexible temperature sensor fabricated using a mixture of CNTs and SnO_2 nanoparticles was investigated. Normally, the performance of a temperature sensor is easily affected by ambient temperature when it is attached to the human skin. To overcome this shortcoming, a polydimethylsiloxane (PDMS) cap with an air cavity, whose depth was 1 mm, covered the top of the device to reduce the environmental effect on temperature sensitivity (Figure 2h inset image). Furthermore, after covered with the PDMS cap, the pressure effect produced by object manipulating on CNT/SnO_2 temperature sensor is reduced because the pressure is mainly distributed on the four edges of PDMS cap. Figure 2h shows that the resistance almost linearly decreased as the temperature increased from 18 to 53.5 °C. The sensitivity extracted from the line fitting was ≈9.84 Ω $°C^{-1}$. The mechanical stability of this temperature sensor was verified by the bending test, in which the resistance value was almost stable at ≈3.18 kΩ (Figure S5, Supporting Information). Furthermore, long-time measurement under different temperatures was also performed to verify the reliable stability and repeatability of this temperature sensor. It is worth to discuss that the protection by PDMS cap makes a side-effect on the recovery process of the temperature sensor. In Figure S6 in the Supporting Information, the result shows the relatively long response (6.4 s) and recovery time (44.4 s) of CNT/SnO_2 temperature sensor. The CNT/SnO_2 temperature sensor exhibited a good fitting result with commercial temperature sensors, which validated the reliability of this device for long-time applications (Figure 2i).

Our skin is sensitive to various stimuli, especially that on the finger tips, which is endowed with abilities of perceiving temperature, touch, pressure, and injuries owing to the densely distributed sensory receptors in the epidermis and dermis.[30] Some of the external stimuli such as cold and nervousness increase the skin wetness that is induced by sympathetic hyperactivity. To figure out the dynamic variation in the finger-skin wetness in response to a cold stimulus, an integrated device that consisted of temperature and humidity sensors was fabricated to simultaneously monitor the skin temperature and humidity, respectively (**Figure 3**a). The humidity-sensor surface was covered by the filter to prevent the ZIS nanosheets from degradation due to the accumulation of water vapor under a high-humidity condition for long time. Although the surface was partially blocked by this filter, the humidity sensor still provided sensitivity that is comparable with a device without protection (Figure S7, Supporting Information). Figure 3b shows that the integrated sensor was attached to the middle finger of the volunteer, and the real-time moisture evaporation level and skin temperature from this finger were monitored wirelessly using a smartphone, which is able to record data from a small microcontroller circuit

board by Bluetooth. The measurement was conducted in two rooms, namely, one at a warm temperature (26 °C) and another at a low temperature (<26 °C), controlled by an air conditioner. During the test, the RH of both rooms was controlled below 35% to reduce interference with the skin moisture.

Initially, the volunteers stayed in the warm room for 10 min to let the body adapt to the warm environment. Then, the volunteers moved to the cold room after 40 s and stayed for another 10 min and finally went back and stayed in the warm room for the final 10 min. This process was repeated to confirm the dynamic skin-wetness change that occurred under a cold stimulus. The resistance-change value of the humidity sensor was converted into RH via calculation using the standard humidity-performance curve shown in Figure S8 in the Supporting Information. Figure 3c shows the monitoring result of the volunteer who experienced a temperature difference of 2 °C during the process. We can clearly see that the finger temperature of this volunteer was maintained at ≈32 °C during 50 min of monitoring, whereas the skin humidity slight fluctuations from 60% to 65%, indicating a normal breathing activity of the skin. In contrast, when the temperature difference in the two rooms increased to 5 °C, both sensors exhibited an evident change when the volunteer moved from the warm (26 °C) to the cold (21 °C) room. Interestingly, the finger-moisture level exhibited a sudden increase (≈10% RH) when the volunteer entered the cold room (21 °C), which indicated a short period of heat loss caused by sympathetic excitation under the cold stimulus (Figure 3d). According to many studies on human skin, the epidermis contains more cold receptors than thermal receptors. Thus, humans are sensitive to cold.[31,32] The finger-skin temperature gradually decreased from ≈30 to ≈19 °C in the first 5 min of stay in the cold room. However, it eventually increased to a medium temperature (≈24 °C) due to the thermoregulation ability of the body. Notably, finger moisture exhibited a decreasing trend with the increase in the finger temperature because the thermoregulator center brought the body temperature back to the normal level by reducing the heat loss from the skin.[5] When this volunteer went back to the warm room, the finger moisture still indicated a slow decrease because the finger temperature took time to recover to the initial value. In the repeat process, an evident increase in the finger-moisture level under a cold stimulus was also observed, which further confirmed the response of the skin when the cold receptors were excited. However, the second response displayed a lower humidity change (≈5%) than the first one (≈10%), which meant that the body has gradually adapted to the tolerable temperature difference using its self-regulation ability.

To accurately investigate the tolerance of the thermoregulator center to higher temperature differences, five volunteers were invited to undergo the same measurement in warm and cold rooms, whose temperatures were set to 26 and 18 °C, respectively. A commercially available thermal IR imager was used to measure the real-time finger temperature. According to the comparison result shown in Figure 3e, the CNT/SnO_2 temperature sensor exhibited a finger temperature that was very near that of the commercial IR imager during the monitoring process in both warm and cold rooms, which indicated the high detection accuracy of this flexible temperature sensor. **Figure 4** shows the monitoring results of the five volunteers at a temperature difference of 8 °C. We can see that all volunteers experienced an increase in the finger-moisture evaporation when they entered the cold room, although their generated finger-moisture levels were different. This result most likely depended on the different distributions of the cold receptors in their bodies, which affected their sensitivity to low temperatures under a cold stimulus. The second volunteer, who experienced an extremely low finger temperature (≈10 °C) during the stay in the cold room, displayed a weak finger-moisture change compared with the other four volunteers. At the same time, the finger temperature of this volunteer was continuously maintained at a very low value (≈15 °C) even after staying in the warm room for 10 min, whereas that of the other four volunteers almost reverted to the original value (≥30 °C) under the same condition (Figure 4b). The abnormal finger temperature and moisture result of the second volunteer revealed a weaker and slower thermoregulation ability of the body.

Among these volunteers, the first one exhibited the highest finger temperature (≈32 °C in the warm room and 23–26 °C in the cold room) as well as fast recovery in her finger temperature to the original value (32 °C) when she moved to the warm room (Figure 4a). Furthermore, the first volunteer easily reduced her finger-moisture level due to the cold stimulus during the finger temperature recovery process, which verified the good thermoregulation ability of her body. Compared with the first volunteer, the finger temperatures of the other volunteers failed to recover to the original value when they stayed in the cold room (18 °C), which were also observed in the repeat process. This result indicated a slower blood flow from the center of the body to the extremities in a colder environment. Simultaneously, to balance the core temperature of the body, the sweat glands gradually reduced the heat loss from the skin; thus, the finger moisture of these volunteers slowly dropped during their long-time stay in the cold environment. Owing to the good thermoregulation ability of the human body, the axillary and forehead temperatures, which represent the core temperature of the body, are stable at a range of 36.2–37 °C (Figure S9, Supporting Information). This stable integrated sensor system presents a high potential in helping people better understand their body and can remind them to keep warm and to exercise to maintain a good physique.

In contrast to the skin in other regions of the body, finger skin plays a significant role in tactile perception and object manipulation. The unique fingerprints on the finger surface, with the finger moisture from the pores, provide our hands a suitable friction between the finger-skin and objects during grasping. When we touch an impermeable surface, the accumulation of the finger moisture in the ridges increases the surface wetness. To visually observe the finger-wetness change during object manipulation, two applications, which included operating a mouse and grasping a smartphone, were investigated. The real-time bending test of this integrated device shows relatively stable outputs of the finger temperature and finger-moisture values even after bending at 180° (Figure S10, Supporting Information). During the mouse-operating process, the finger temperature did not change, whereas the humidity sensor exhibited an evident decrease in the resistance-change ratio owing to the accumulation of finger-skin wetness (**Figure 5**a–c). To exclude the resistance change of ZIS humidity sensor caused by pressure, the pressure test was conducted. It is evident that the ZIS humidity sensor shows only less than 1% of resistance change even at high pressure value of 1.7 kPa (Figure S11, Supporting Information). It should be noted

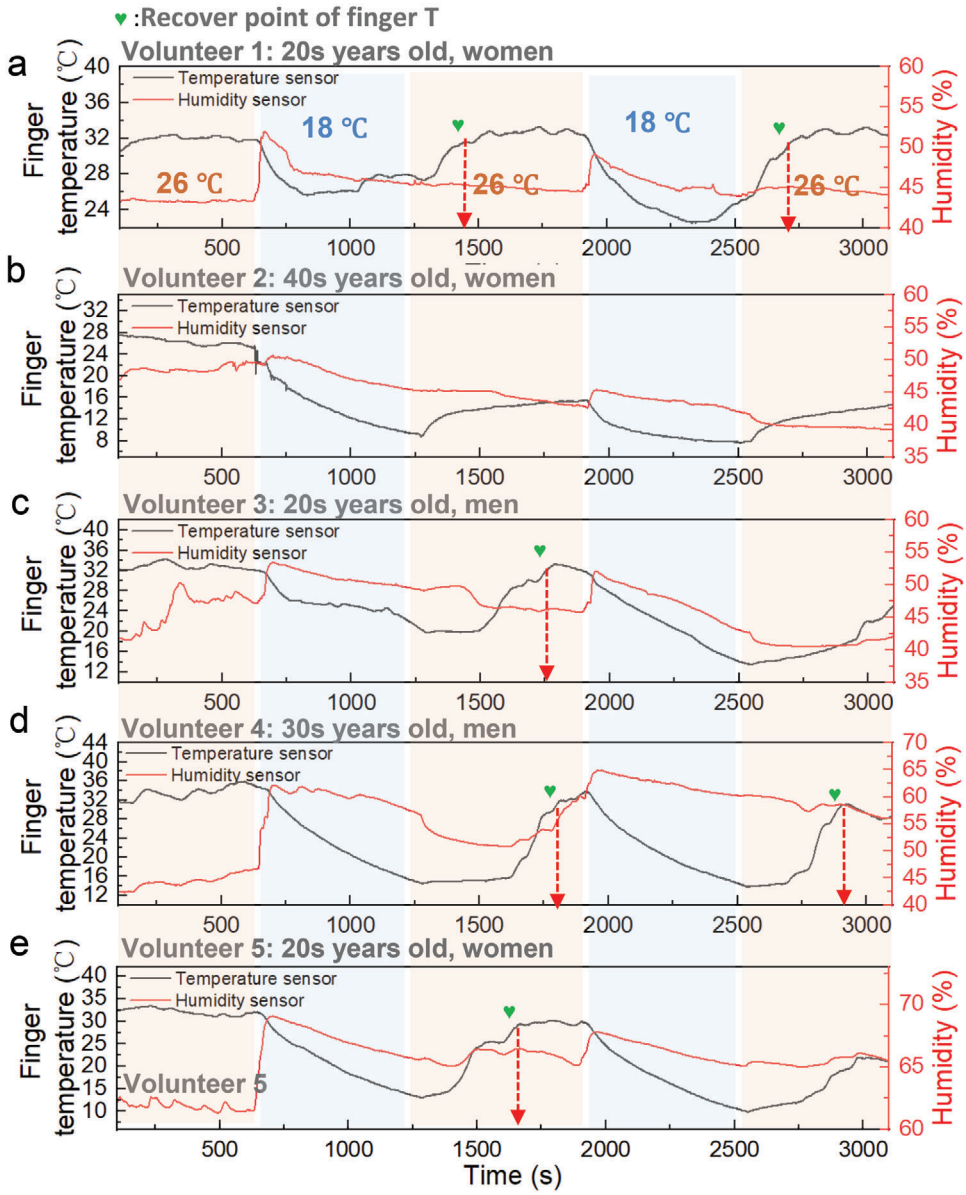

Figure 4. a–e) Real-time monitoring of the finger temperature and moisture of the five volunteers in the cold-stimulus test.

that pressure application up to only 1.7 kPa was tested because the demonstrations shown in Figure 5 were affected by this pressure range under manipulation of small items like a smartphone and a mouse. In general, too high or too low finger-skin wetness usually results in object slipping. The result in Figure 5c shows that the finger-moisture level could reach a saturated value during 1 min of mouse manipulation, indicating controllable skin wetness through the fingerprint structure. Similarly, the finger moisture also exhibited an obvious increase (≈2–3% RH) during grasping a smartphone, although the humidity sensor displayed a relatively slow recovery in the resistance change after releasing the smartphone (Figure 5d–f). Precise manipulation of different objects is attributed to the nature the fingerprint structure and adjustable finger-skin wetness, which are beneficial for enhancement of the friction between the hands and objects.

The skin-moisture level indirectly predicts the health status of a human body through its response by the operation of the thermoregulation center, which is important for maintaining a stable body temperature during various human activities, including having hot meals and doing exercises. Without dynamic skin-moisture evaporation from the sweat glands, the body temperature tends to run out of control, which can finally lead to serious diseases. Thus, studying the dynamic variation in the skin-moisture level is necessary to prevent potential diseases resulting from thermoregulatory disorder. Figure 5g shows both the finger temperature and finger moisture of a healthy adult when eating hot noodles. To reduce the environmental humidity effect on humidity sensor, this device was assembled in a wearable glove and worn on the left hand of the volunteer. It is obvious that the finger temperature gradually increases from 28 to 32 °C during this

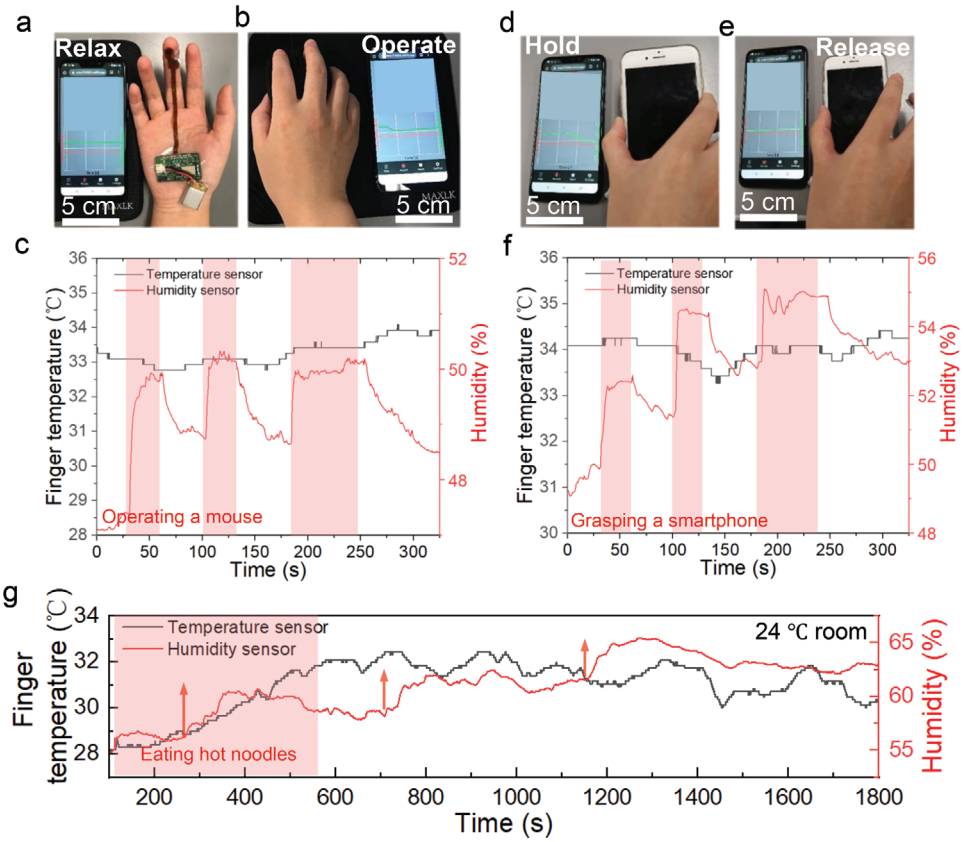

Figure 5. Photograph and monitoring results of the finger wetness while a–c) operating a mouse and d–f) holding a smartphone. g) Monitoring results of the finger temperature and moisture level as a form of heat production and dissipation during eating of hot noodles.

process and remains at a high value (>30 °C) for ≈20 min after eating. Simultaneously, the finger moisture shows three periods of increases (a total of ≈8% RH) during and after eating noodles (these periods are highlighted by the red arrows in Figure 5g), which indicates a normal heat-dissipation process as the body temperature increases.

However, the sensitivity to hot or cold in each person is different because of the unique distributions of the thermal receptors in their bodies. To determine the dynamic skin temperature and skin-moisture variation of different people, the real-time monitoring results of five volunteers who run twice (5 and 10 min; speed: 7 km h^{-1}) were compared. In this study, the integrated device was put inside a cotton glove by sewing it into a linen cloth, which was more comfortable and breathable for the users. Although the finger moisture was slightly blocked by the linen cloth, the result of the ZIS humidity sensor still exhibited an evident peak-to-peak difference during the wearing and taking off of the glove, which was similar to that of a bare finger. However, almost no resistance change was observed when a plastic glove was worn (Figure S12, Supporting Information). **Figure 6**a–c shows the glove where the assembled device was worn on the right hand of the volunteer who performed the running test on a commercial treadmill. Figure 6d–h shows the monitoring results of the five volunteers at different ages. The sweating condition of each person is also labeled. All volunteers drank sufficient water before running to prevent body dehydration. During the first 5 min of running, the first volunteer, who exhibited a good thermoregulation ability in the cold-stimulus test, experienced dramatic increases in both finger moisture (≈25%) and finger temperature (≈6 °C) (Figure 6d). During rest, the finger-moisture level dropped to a lower value to save the water content in the body; however, it increased again when the second running test was performed. This result verified that our thermoregulation center mainly maintains a stable body temperature by balancing the heat production in vivo and heat loss in vitro during running. Compared with those in the other volunteers, the finger temperature of the first volunteer was maintained at a high value until the end of her rest, which indicated that the heat produced by the muscle mass metabolism was higher than the heat released by the thermoregulation center in her body. Simultaneously, the sweating points of the first volunteer appeared earlier than those of the others, which matched well with her higher body temperature than those of the others during running. The fifth volunteer also experienced a mild increase in the finger temperature, whereas the remaining three volunteers exhibited an opposite condition during running, which could be owing to the slower responses of their heat-production center (Figure 6h). Thus, the second, third, and fourth volunteers experienced increased finger temperature only at rest during which the evaporation of the finger moisture was also enhanced. However, all volunteers exhibited different sweating conditions irrespective of the sweating time or volume due to not only the different numbers of sweat

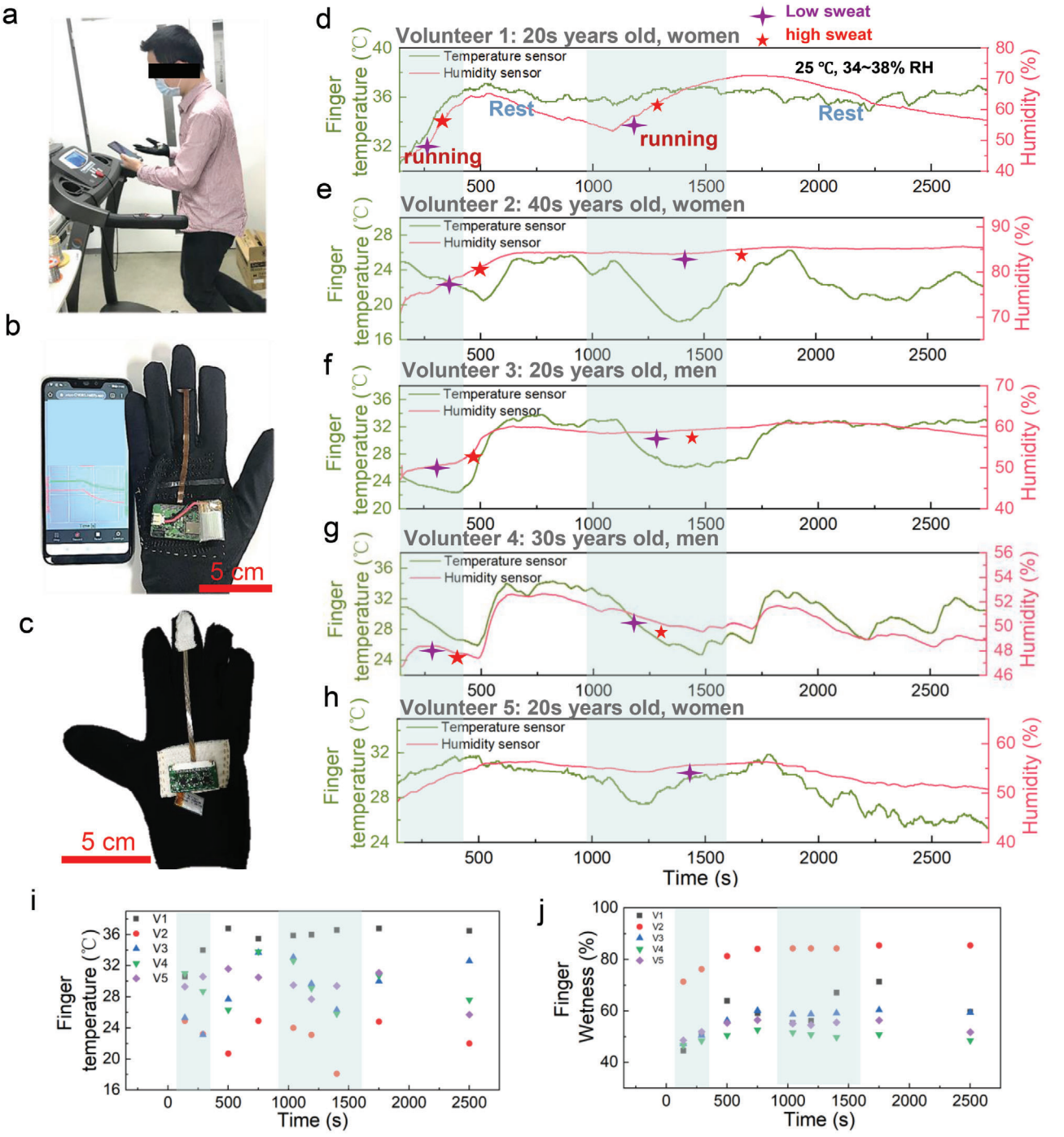

Figure 6. a) Photograph of a volunteer who performed the running experiments on a treadmill. b,c) Photographs of the wireless monitoring of the finger temperature and moisture evaporation using a glove-based device. d–h) Real-time finger temperature and moisture monitoring results of the five volunteers who ran twice at a speed of 7 km h^{-1} during the test. The two running processes took 5 and 10 min. Summarized i) finger temperature and j) finger-wetness variation of the five volunteers in the running test.

glands distributed on their skins, but also the effect of the coordination of the heat-producing and heat-dissipating centers in their body.

To observe the difference in the monitoring results, the collected data were summarized. Figure 6i,j shows the comparison of the finger temperature and finger-moisture level of the five volunteers, respectively. Figure 6i shows that the first volunteer demonstrated the highest finger temperature, whereas the second volunteer demonstrated the lowest. According to the cold-stimulus test shown in Figure 4, the second volunteer, who possessed relatively weak thermoregulation ability, also demonstrated a low finger temperature during running (≈18–25

°C). Simultaneously, according to the highest finger-moisture level of the second volunteer (≈70–85% RH) shown in Figure 6j, the fast heat dissipation of her body is confirmed. Obviously, the other volunteers demonstrated a similar trend variation in the finger-moisture level in the running experiment. In general, the integrated sensor system that consisted of a ZIS humidity sensor and a CNT/SnO_2 temperature sensor successfully achieved long-time monitoring of the finger-moisture level and finger temperature, respectively. The results from the five volunteers illustrated the dynamic activities of their thermoregulator centers, which present a new path for human health care through observation of their physical signals under different situations.

3. Conclusion

In summary, an integrated flexible sensor system with a $ZnIn_2S_4$ nanosheet-based humidity sensor and a CNT/SnO_2 temperature sensor has been designed for wireless monitoring of the finger temperature and finger moisture during different activities. Both sensors demonstrated reliable sensitivity and stability during the cyclic test compared with the commercial humidity and temperature sensors. Owing to the natural sensitivity of the finger skin to thermal perception, an evident increase in the skin-moisture level was observed during the measurement of the performance of the five volunteers, who experienced a temperature difference of 8 °C when they moved from a warm (26 °C) to a cold (18 °C) room. The evident secretion by the sweat glands mainly stemmed from the excitation of the sympathetic nerve in the human body.

The finger wetness that resulted from the mechanical touch by using this sensor system was also observed when a volunteer operated a mouse and held a smartphone. Furthermore, the moisture evaporation from the finger skin of these five volunteers was investigated during running when the thermoregulator center was more active because of the increase in heat production due to the muscle contraction during the exercise. Interestingly, the finger temperature of the three volunteers (Volunteers 2–4) exhibited different degrees of reduction as well as a mild increase in the finger moisture, which displayed a slow and weak thermoregulation process during running. In other words, because of the slow heat generation of their muscles, the heat-dissipation center only exhibited a small response to thermal balance in their bodies. However, the first volunteer showed a dramatic increase in both finger temperature and finger moisture under the same condition, which indicated the fast metabolism of her body during exercise. The proposed flexible integrated sensor system provides a new approach for disease diagnosis by monitoring the activities of the thermoregulator center in our body. For further precise analyses, there are several challenges to be addressed for the sensor. One is the relatively slow response and recovery process of both sensors remains to be resolved due to the reflection of evident hysteresis. However, the sensor outputs for both humidity and temperature sensors return to the initial value at low humidity and low temperature for the cycle test. These results suggest that the sensors have less hysteresis for a long-time monitoring. We should note that further studies by investigating more volunteers are necessary to understand the thermoregulator center and confirm its performance based on the skin wetness and temperature. This flexible sensor system provides a high potential path of pre-diagnosing human diseases such as fever, hyperthyroidism, and hypothermia, which are aroused by thermoregulation center disorders. In the future, more sensors such as pH and chemical sensors will be investigated to further improve the detection range and accuracy according to the targeted disease. When all physiological experiments will be conducted in the future, this sensor system may provide a new application for wearable sensors in disease risk prediction during abnormal thermoregulation process in the human body, which can promote the development of a healthy diet and suitable exercise habit for every person.

4. Experimental Section

Synthesis of $ZnIn_2S_4$ Nanosheets: First, 1 mmol $ZnCl_3$ (Sigma-Aldrich, 99.999% trace metal basis), 0.5 mmol $InCl_3{\cdot}4H_2O$ (Sigma-Aldrich, 97%), and 2 mmol thioacetamide (Sigma-Aldrich, ≥99%) were mixed in deionized (DI) water by continuous stirring for ≈15 min. Then, the mixture was stirred and heated in a water bath at a constant temperature of 95 °C for ≈5 h. Finally, the product was washed three times with DI water and prepared into a concentration of 10 mg mL^{-1}. In this work, "ZIS" was used as the abbreviated name for $ZnIn_2S_4$ nanosheets.

Device Fabrication: The ZIS humidity sensor was composed of interdigital LIG electrodes and a ZIS nanosheet film. The porous graphene electrodes were fabricated using laser scanning (power: 3 W; speed: 50 cm s^{-1}) on a clean polyimide (PI) film (thickness: 50 µm). Subsequently, the LIG electrodes on the PI film were cleaned by gentle blowing using N_2 gas. Then, 30 µL of ZIS nanosheet solution was drop-casted and annealed onto the LIG electrodes at 100 °C for 20 min. To ensure stable output of this humidity sensor during measurements, the end of the graphene electrodes was coated using a silver paste, which was annealed at 70 °C for 30 min. Finally, the surface of the humidity sensor was covered by a porous waterproof breathable film (TEMISH, Nitto Denko) to protect the ZIS film from degradation. The waterproof test is shown in Figure S13 in the Supporting Information.

The CNT/SnO_2 temperature sensor was fabricated according to the following processes. First, silver electrodes were screen-printed on a polyethylene terephthalate (PET) film (38 µm) and baked at 70 °C for 1 h. Then, a single-walled CNT solution (20 µL, concentration: 0.01%) and SnO_2 nanoparticles (40 mg, Sigma-Aldrich, ≤100 nm) were uniformly dispersed in DI water (4 mL) by continuous stirring. The prepared mixture was then drop-casted on the silver electrodes and annealed at 110 °C for 10 min. Thereafter, the device was flushed using hot water for 3 min to remove the impurities on the surface, followed by overnight baking at 90 °C. Finally, the temperature sensor was coated with a passivation layer (SIFEL2661, Shin-Etsu Chemical, Japan) to prevent the influence of gas and humidity from outside. To consider the effect of ambient temperature on the CNT/SnO_2 temperature sensor during skin-temperature monitoring, the top of this sensor was covered by a PDMS cap (length: 6 mm; width: 3 mm; height: 2 mm) with an air cavity (depth: 1 mm) using the PDMS connection.

The fabrication process of the integrated device is described as follows. Silver electrodes were first screen-printed on a PI film (50 µm). Next, the CNT/SnO_2 temperature sensor was attached onto the silver electrodes using a silver paste and baked at 90 °C for 3 h. Then, the interdigital LIG electrodes were manufactured by laser scanning at a good alignment with the silver electrodes. The ends of the exposed LIG electrodes were coated with a silver paste to create a good connection with the silver electrodes. Finally, the humidity-sensor part was completed after the ZIS nanosheet solution was drop-casted on the LIG electrodes and the top of the device was covered by a waterproof breathable membrane filter.

Characterization: The surface morphology images were characterized using a Hitachi S-4300 scanning electron microscope (SEM). Raman characterization was conducted using a HORIBA Raman spectrometer (Labram HR Evolution). The fundamental experiments of the ZIS humidity sensor were performed in a humidity- and temperature-controllable oven (Espec, SH-222), which was equipped with a multi-channel data logger

(Hioki, LR8400) that was used for data collection. During the measurements, commercial humidity and temperature sensors were installed in parallel in the oven to calibrate the RH and temperature. The calibration result of the finger-skin temperature at different temperatures was recorded using an IR camera (Keysight Technologies, TrueIR). The measurements of the finger wetness at different temperatures were carried out in two different rooms that were set to warm (26 °C) and cold (18–24 °C) modes using an air conditioner. During the wireless monitoring, the integrated device was connected to a printed circuit board that was charged by a lithium-ion battery. Simultaneously, the data were collected by a smartphone via wireless communication. The wireless monitoring of the finger wetness during running was performed on a commercial treadmill (IGNIO, shock-absorbing system).

Physiological Experiment: The experiments for the monitoring of the skin wetness and temperature by attaching the sensor system on the skin were performed in compliance with the protocol approved by the ethical committee at Osaka Prefecture University. Informed consents from all volunteers to record and use all data were obtained.

Statistics: The number of subjects were 5, and all data are reported in figures. Temperature and humidity values were extracted from the calibration curves of each sensor. There is no statistic calculation or analyses in this study.

Supporting Information

Supporting Information is available from the Wiley Online Library or from the author.

Acknowledgements

This work was supported by JST PRESTO (JPMJPR17J5), JSPS KAKENHI grants (JP17H04926 and JP18H05472), JST Accelerated Program (JPMJCR21U1), and the TEPCO Memorial Foundation. K.X. was supported by JSPS International Research Fellowship.

Conflict of Interest

Y.L. and K.T. are inventors of a patent filed for the humidity sensor.

Data Availability Statement

The data that support the findings of this study are available on request from the corresponding author. The data are not publicly available due to privacy or ethical restrictions.

Keywords

flexible humidity sensors, flexible temperature sensors, skin wetness, thermoregulatory, wearable devices

Received: January 17, 2021
Revised: April 14, 2021
Published online:

[1] D. Filingeri, R. Ackerley, *J. Neurophysiol.* **2017**, *117*, 1761.
[2] M. Wang, Y. Luo, T. Wang, C. Wan, L. Pan, S. Pan, K. He, A. Neo, X. Chen, *Adv. Mater.* **2020**, 2003014 https://doi.org/10.1002/adma.202003014.
[3] K. Xu, Y. Lu, K. Takei, *Adv. Funct. Mater.* **2021**, 2007436 https://doi.org/10.1002/adfm.202007436.
[4] G. Yao, L. Xu, X. Cheng, Y. Li, X. Huang, W. Guo, S. Liu, Z. L. Wang, H. Wu, *Adv. Funct. Mater.* **2020**, *30*, 1907312.
[5] D. Filingeri, N. B. Morris, O. Jay, *Exp. Physiol.* **2017**, *102*, 100.
[6] K. Tsuzuki, Y. Mochizuki, K. Maeda, Y. Nabeshima, T. Ohata, V. Draganova, *Energy Build.* **2020**, *207*, 109562.
[7] C. C. S. Tan, L. K. K. Chin, I. C. C. Low, *Proteomics* **2020**, *20*, 1800468.
[8] S. Racinais, S. Cocking, J. D. Périard, *Temperature* **2017**, *4*, 227.
[9] H. Kim, Y. S. Kim, M. Mahmood, S. Kwon, N. Zavanelli, H. S. Kim, Y. S. Rim, F. Epps, W. H. Yeo, *Adv. Sci.* **2020**, *7*, 2000810.
[10] S. Lee, S. Franklin, F. A. Hassani, T. Yokota, M. O. G. Nayeem, Y. Wang, R. Leib, G. Cheng, D. W. Franklin, T. Someya, *Science* **2020**, *370*, 966.
[11] Y. Yang, Y. Song, X. Bo, J. Min, O. S. Pak, L. Zhu, M. Wang, J. Tu, A. Kogan, H. Zhang, T. K. Hsiai, Z. Li, W. Gao, *Nat. Biotechnol.* **2020**, *38*, 217.
[12] M. Bariya, H. Y. Y. Nyein, A. Javey, *Nat. Electron.* **2018**, *1*, 160.
[13] R. Chen, Z. Zhu, S. Ji, Z. Geng, Q. Hou, X. Sun, X. Fu, *Biomaterials* **2020**, *255*, 120201.
[14] A. Nemcova, M. Seitl, T. Dominik, M. Semela, M. Sucha, R. Kolar, V. Svozilova, K. Bucsuhazy, R. Smisek, M. Mezl, B. Hesko, M. Belak, M. Bilik, P. Maxera, *IEEE Trans. Intell. Transp. Syst.* **2020**, *1*, 2977762.
[15] Y. Lu, K. Xu, L. Zhang, M. Deguchi, H. Shishido, T. Arie, R. Pan, A. Hayashi, L. Shen, S. Akita, K. Takei, *ACS Nano* **2020**, *14*, 10966.
[16] K. Xu, Y. Lu, T. Yamaguchi, T. Arie, S. Akita, K. Takei, *ACS Nano* **2019**, *13*, 14348.
[17] S. Nakata, M. Shiomi, Y. Fujita, T. Arie, S. Akita, K. Takei, *Nat. Electron.* **2018**, *1*, 596.
[18] G. Mattana, T. Kinkeldei, D. Leuenberger, C. Ataman, J. J. Ruan, F. Molina-Lopez, A. V. Quintero, G. Nisato, G. Tröster, D. Briand, N. F. d. Rooij, *IEEE Sens. J.* **2013**, *13*, 3901.
[19] G. Rosace, V. Trovato, C. Colleoni, M. Caldara, V. Re, M. Brucale, E. Piperopoulos, E. Mastronardo, C. Milone, G. De Luca, M. R. Plutino, *Sens. Actuators, B* **2017**, *252*, 428.
[20] N. Gerrett, Y. Ouzzahra, B. Redortier, T. Voelcker, G. Havenith, *Physiol. Behav.* **2015**, *152*, 11.
[21] K. C. Kregel, D. R. Seals, R. Callister, *J. Physiol.* **1992**, *454*, 359.
[22] K. Hamunen, V. Kontinen, E. Hakala, P. Talke, M. Paloheimo, E. Kalso, *Br. J. Anaesth.* **2012**, *108*, 838.
[23] T. Miyake, S. Nakamura, M. Zhao, K. So, K. Inoue, T. Numata, N. Takahashi, H. Shirakawa, Y. Mori, T. Nakagawa, S. Kaneko, *Nat. Commun.* **2016**, *7*, 12840.
[24] D. Filingeri, H. Zhang, E. A. Arens, *J. Appl. Physiol.* **2018**, *125*, 723.
[25] R. Paricio-Montesinos, F. Schwaller, A. Udhayachandran, F. Rau, J. Walcher, R. Evangelista, J. Vriens, T. Voets, J. F. A. Poulet, G. R. Lewin, *Neuron* **2020**, *106*, 830.
[26] L.-T. Wang, H.-H. Wang, H.-C. Chiang, L.-Y. Huang, S.-K. Chiu, L. K. Siu, K.-J. Liu, M.-L. Yen, B. L. Yen, *Cell Rep.* **2020**, *32*, 108188.
[27] K. Xu, Y. Fujita, Y. Lu, S. Honda, M. Shiomi, T. Arie, S. Akita, K. Takei, *Adv. Mater.* **2021**, 2008701 https://doi.org/10.1002/adma.202008701.
[28] Y. Lu, K. Xu, M.-Q. Yang, S.-Y. Tang, T.-Y. Yang, Y. Fujita, S. Honda, T. Arie, S. Akita, Y.-L. Chueh, K. Takei, *Nanoscale Horiz.* **2021**, *6*, 260.
[29] Y. Xie, Y. Liu, H. Cui, W. Zhao, C. Yang, F. Huang, *J. Power Sources* **2014**, *265*, 62.
[30] I. You, D. G. Mackanic, N. Matsuhisa, J. Kang, J. Kwon, L. Beker, J. Mun, W. Suh, T. Y. Kim, J. B.-H. Tok, Z. Bao, U. Jeong, *Science* **2020**, *370*, 961.
[31] Q. Wu, J. Liu, L. Zhang, J. Zhang, L. Jiang, *Build. Environ.* **2020**, *171*, 106640.
[32] D. Schmidt, G. Schlee, T. L. Milani, A. M. C. Germano, *J. Therm. Biol.* **2020**, *93*, 102718.

